




# Computer aided detection of mercury heavy metal intoxicated fish: an application of machine vision and artificial intelligence technique

Ritesh Maurya<sup>1</sup> · Arti Srivastava<sup>2</sup> · Ashutosh Srivastava<sup>2,3</sup> · Vinay Kumar Pathak<sup>4</sup> · Malay Kishore Dutta<sup>5</sup> 

Received: 25 March 2021 / Revised: 12 November 2022 / Accepted: 2 January 2023 /  
Published online: 10 January 2023

© The Author(s), under exclusive licence to Springer Science+Business Media, LLC, part of Springer Nature 2023

## Abstract

Heavy metal pollution in our aquatic bodies is a major health concern in the present scenario. The harmful effect of non-biodegradable toxic and trace metals is more serious than other contaminants. Fishes are more susceptible to various harmful impacts of these pollutants within the aquatic environment. Heavy metal toxicity from fish intake can cause health problems such as multi-organ damage, and serious diseases. Due to bioaccumulation through the food chain and direct absorption of these heavy metals, it is very important to monitor the quality of food fishes. Classical chemical-based methods for the assessment of fish quality are destructive and at the same time, they also require costly machines and expert manpower. In the present work, a machine learning-based methodology has been employed in which the suitable color and texture features have been identified and have been genetically optimised for the classification of heavy metal exposed and non-exposed fish using a machine learning classifier. The performance of the proposed method has also been tested using transfer learning-based approach. The best F1-score of 97.1% and 93.5% have been obtained in the case of the proposed genetically optimised color texture features-based approach and the transfer learning-based approach respectively. Thus, the proposed technique can be utilised to identify heavy metal-contaminated fish and to mitigate possible consequences. The proposed method can also be used for large-scale fish processing.

**Keywords** Center initialised K-means algorithm · Convolutional neural network · Deep learning · Heavy metal intoxicated fish · Transfer learning

---

✉ Malay Kishore Dutta  
malaykishoredutta@gmail.com

## 1 Introduction

Heavy metals are natural constituents of marine environments; however, their levels have been continuously rising in recent years due to geological weathering, various anthropogenic activities such as the discharge of agricultural, municipal and industrial wastes, and direct atmospheric deposition [13, 35]. Earlier researchers have found that there is an increase in the pollution of specific heavy metals in freshwater systems around the world, notably rivers. Industrial operations and trash have been the primary sources of pollution [22, 29]. Toxic metals have affected freshwater ecosystems all around the world [12, 44]. Many studies have been organised in the past to examine the effects of heavy metals on various fish species [10, 38]. These findings highlight the key necessity of monitoring heavy metal levels in fish species to improve freshwater ecosystems [24]. Heavy metals are known to have negative implications for human health when passing through the food chain [31]. Heavy metals can also cause histopathological abnormalities in the internal structure of the gills and brain [5]. The consumption of these heavy metal-intoxicated fish can cause detrimental hazards to human health [3]. As fish is a daily food for billions in the world, it is a huge challenge for the aquaculture industry to keep track of the quality of fish for safe human consumption [11]. Heavy metal toxicity has a negative impact on the fish quality [25].

Heavy metals can be propagated into fish either through the alimentary tract or through gills or skin [49]. Then, absorbed heavy metals are transported through the bloodstream of fish to other organs and tissues, where they get bioaccumulated [19]. The bioaccumulation of heavy metals like Cd, Pb, Cu, Fe, Zn, Mn, Hg, and As in fish occurs in the liver, gills, and skin tissues [41]. Lead, cadmium, mercury and arsenic heavy metals are the main threat to human health. The harmful effects of these heavy metals have been periodically reviewed by international bodies such as WHO [28]. These heavy metals also destroy the metabolic process in human beings [20]. Other risks such as cardiovascular disorders, renal damage, cancer and diabetes are also associated with drinking contaminated water [42].

In [14], the level of exposure to mercury (Hg), lead (Pb), and cadmium (Cd) in adult population was investigated. Mercury (Hg) was found to be present in high concentration in sea foods in comparison to other Heavy metals (Cd, Hg, and Pb). In another study, probable sources of heavy metal contamination in fish through bioaccumulation have been studied to evaluate possible human health risks. It was found that gills have a high concentration of heavy metals in collected fish samples [37]. A similar pattern of bioaccumulation was also found in different species of fish found in various regions of the world [56]. Since fishes are in direct contact with water, gills are more prone to bio-accumulation [43]. Therefore, gills are considered the main area of investigation for the present study.

The classical methods for the categorisation of heavy metals exposed fish are based on the chemical testing method such as inductively coupled plasma mass spectrometry (ICP-MS), Liquid chromatography-mass spectrometry (LC-MS), and High-Performance Liquid Chromatography (HPLC). Identification and detection of heavy metal contamination in fish is a challenging task and these conventional methods need several costly devices, chemicals, laboratories and expert manpower. These techniques are also highly time-consuming, costly, and destructive, since, the sample under chemical testing becomes unusable [8]. Hence, there exist a playing field to thrive into an automatic and non-invasive method for the identification of heavy metal exposure to fish.

The advent of artificial intelligence brings a huge transformation in research and development to provide intelligent assistance and decision-making [33, 51, 59]. Machine learning

classifiers and convolutional neural networks (CNNs) have recently been used in the many applications of different domains such as object classification [30], medical image analysis [34], biology [2, 7], medicine [9], and bioinformatics [39]. CNN is one of the most popular models for image processing for two reasons: there is no need for manual analysis of the features. Another reason being the models acts as a feature extractor as well as a classifier.

In the proposed work, colour and texture-based features optimised with the genetic algorithm have been used for the classification of fish sample images. The performance obtained with the proposed color and texture features-based genetically optimised feature selection method has been compared with the transfer learning-based-deep feature extraction and classification method. The proposed method at first, segments the gill region using the customised K-means clustering algorithm, and then the color and texture features extracted from the segmented gill region were fused. The fused features were further optimised using the fitness function defined for the genetic algorithm. Finally, the final classification results obtained with the classical machine learning classifiers have been compared with the state-of-the-art transfer learning-based approach. Both methods have been compared extensively to different performance metrics to prove the effectiveness of the proposed former color texture feature-based method in comparison to the deep feature-based method. The main contributions made by the present work can be summarised as follows:

- (i) An automatic cost-effective and non-destructive machine learning-based methodology has been proposed for the categorisation of normal (non-exposed) and heavy metal exposed fish.
- (ii) Suitable color and texture features have been identified that discriminate the heavy metal-exposed and non-exposed fish.
- (iii) Extracted color texture features have been optimised using the genetic algorithm for better performance.

Though the scope of the present study is limited to the identification of mercury-heavy metal exposed fish identification it can be extended to other heavy metals as well.

The rest of the paper can be systematically studied in the following fashion: Section 2 briefs the most relevant related works. Section 3 explains the materials and methods used in the present work. Section 4 presents experimental results and carries out discussions on the experimental outcomes. Section 5 compares the present work with other related works. Finally, Section 6 concludes.

## 2 Related works

This section summarises some research and development of new techniques which has been used to assess the different aspects of fish related issues. For the detection of heavy metals in fish tissue, a microfluidic device-based colorimetric sensor device with a highly sensitive enzyme nanoprobe has been constructed. However, nanoprobe of this type had to be stored in certain settings to be preserved. Typical devices still rely on microscopes or other readout technologies, which are challenging to include in on-site portable tests. As a result, standalone systems must be developed using new technologies to enable the creation of practical analytical platforms [54]. Furthermore, numerous previous research studies have indicated

trends towards sophisticated mercury sensors-based paradigm to the active participation of state-of-the-art artificial intelligence and machine learning-based systems [32].

Image processing techniques have widely been adopted in different studies to estimate the quality of fish and exposure to toxic elements. An image processing-based framework had been presented for the evaluation of the wholesomeness of a fish using wavelet features extracted from fish gills [17]. In another work, the freshness of a fish was evaluated by analysing the changes that took place in the colour of an eye and a gill tissue [16]. Various image processing-based methods were also summarised for the assessment of fish quality and freshness [15]. Computer vision-based techniques are also studied for the quality assessment of the fish exposed to pesticides [47]. A method for identifying heavy metal-exposed fish was designed with an image processing and machine learning techniques with gills tissue as the key region of interest (ROI). The AUC value for identifying metal-exposed fish using a classification tree range from 82% to 92% [53]. Evolutionary algorithms have also been used to find the optimal set of features [26]. Sengar et al. have used the image processing-based method to analyse the freshness of a fish. They have analysed the statistical features extracted from the fish skin tissue image in HSV (Hue, Saturation, Value) colour space [48]. Banwari et al. have used the fish eyes as a region of interest and established a relation between the eye colour and storage pattern of a fish to assess the freshness of the fish sample [4].

The present work proposes a color texture feature extraction-based method in which the extracted features are optimised genetically. The genetically optimised features present better generalisation and classification accuracy due to the small number of selected features. The performance of the proposed method has been compared and analysed with the transfer learning-based method.

### 3 Materials and methods

#### 3.1 Experimentation details

Freshwater fish *Channa punctatus* were collected from the fish farm at Noida, Uttar Pradesh. *C. punctatus*, a freshwater fish belonging to the Channidae family, is also referred to as the snake-headed murel. This fish is local to India and a few other nations in the region. Certain biological characteristics that distinguish the fish as an ideal model include a wider distribution range, sensitivity to environmental toxins, ease of transportation, and maintenance in laboratory settings [50]. The average weight of the fish was  $20 \pm 2.0$  g and the average length was  $12 \pm 0.5$  cm. All fishes were kept in the 100 L glass aquarium (10 fishes per aquarium) filled with dechlorinated water at room temperature for 15 days. LC50 (96 h), in case of, mercuric chloride was measured using Boyd's method [6]. Post acclimatization, fish were distributed into two classes. The first class (100 fishes) was exposed to mercuric chloride (0.10 mg/l – sublethal dose), and the second class (100 fishes) was treated as a control without any metal exposure. Fishes in the exposed group were exposed to a sublethal dose of mercury for 15 days. To keep up the concentration of metal in tanks, water in the tank was renewed daily. Water quality parameters like temperature pH and dissolved oxygen were maintained at  $24 \pm 2^\circ$  C,  $7.5 \pm 0.1$  and  $5.5 \pm 0.2$  mg/L, respectively.

Fishes were anaesthetized by immersing in the solution of tricaine methane sulphonate (MS 222) (25 mg/l) for 3–5 minutes after 15 days of metal exposure. Post-acquisition of the image of fish gill, fish were dissected to preserve liver tissue for mercury estimation. 100 mg of liver tissue was exposed to 1 ml of concentrated nitric acid (water diluted) at  $80^\circ$  C for an hour.

Perkin Elmer AA800 (Atomic Absorption Spectrophotometer) was deployed to estimate the presence of Hg in liver. Table 1 shows precisely the concentration of metal in the liver of fish exposed to mercuric chloride for 15 days.

### 3.1.1 Image acquisition

The 20.2. MP (megapixel) Canon IXUS 285HS digital camera has been used to capture the fish sample images. The camera has been hung from the roof of a wooden box of dimension 100X120X100 (in centimetres) and placed at a distance of 8 cm from the fish specimen. The box has been illumination with four CFLs (25 W), three tube lights each of 9 W and three LED (Light-emitting diodes) lamps (18 W) placed at a 45-degree angle to uniformly illuminate the fish sample placed under them. The acquired sample image is of size 3885X5814 pixels. The schematic representation of the image acquisition setup has been shown in Fig. 1.

## 3.2 Proposed methodology

The proposed methodology consists of the following steps: (i) Acquisition of fish-sample image (ii) Segmentation of the Region of Interest i.e., gill (iii) feature extraction (iv) Classification of heavy-metal exposed and non-exposed fish using genetically optimised color texture features. The proposed methodology for the current proposed work has been presented using Fig. 2. In stage I, the collected fish samples are first categorised into two groups – The exposed group and the control group. Then, images of these fish samples were passed through various image processing operations like color space conversion and clustering to segment out the gill region in stage II. In stage III, the color and textural features drawn out from the segmented gill image are given to the classifier after selecting the optimised features using a genetic algorithm. In stage IV, these extracted features are given as input to different classifiers and these classifiers after subsequent training are used for testing unseen test samples to check the efficacy of the proposed classification approaches.

### 3.2.1 Fish gill segmentation

Gill is a red-coloured respiratory organ in the fish through which blood flows directly. The colour of the fish gills varies physically, and these changes yield discriminatory characteristics, which were exploited in the proposed work. Because the proposed work involves image analysis, parameters that are easily detectable using computer vision techniques should be chosen. As a result, the gills were chosen as the region of interest in the suggested technique.

An input fish image is being analysed in different colour models for segmentation of the gill as a Region of Interest with better visibility. YCbCr color model has been used for input image processing the reason for choosing the YCbCr color model has also been described in the next subsection.

**Table 1** Bioaccumulation of heavy metals in the liver of fish

Class/Group	Metal concentration ( $\mu\text{g/g}$ ) (Mean $\pm$ Std. Deviation)
Control group	Not detected
Hg exposed group	0.73 $\pm$ 0.7

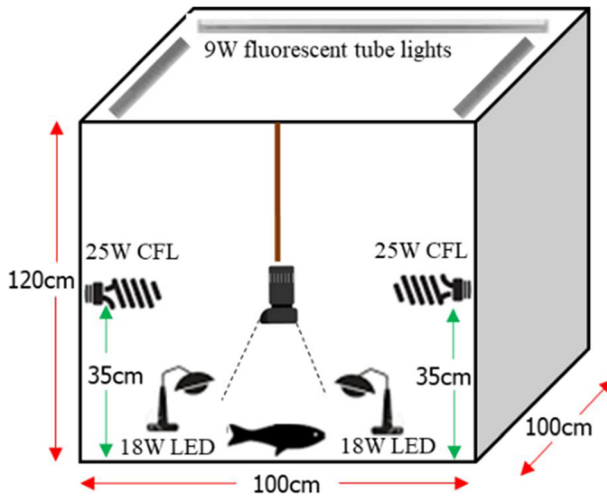


Fig. 1 The schematic representation of the fish sample image acquisition setup

**YCbCr color model** The fish image acquired from the camera is in the RGB (red green and blue) color format. The RGB color model is not appropriate for gill segmentation because this model does not work well for color-based detection as this model mixes the color (chrominance) and intensity (luminance) information present in an input image. Further, after converting the input image from RGB to the YCbCr color model, it was observed that the chrominance component of the YCbCr color model represents the marked similarity between the gills of different fish samples which can be used to distinguish the gill region from the rest of the fish body. Another reason, for selecting the YCbCr model is that the YCbCr model works well in medium light conditions. The mathematical model for the conversion of the RGB model to the YCbCr model is performed using Eq. (1) as follows:

$$\begin{bmatrix} Y \\ C_b \\ C_r \end{bmatrix} = \begin{bmatrix} 0.257 & 0.504 & 0.098 \\ -0.148 & -0.219 & 0.439 \\ 0.439 & -0.368 & -0.071 \end{bmatrix} \begin{bmatrix} R \\ G \\ B \end{bmatrix} + \begin{bmatrix} 16 \\ 128 \\ 128 \end{bmatrix} \quad (1)$$

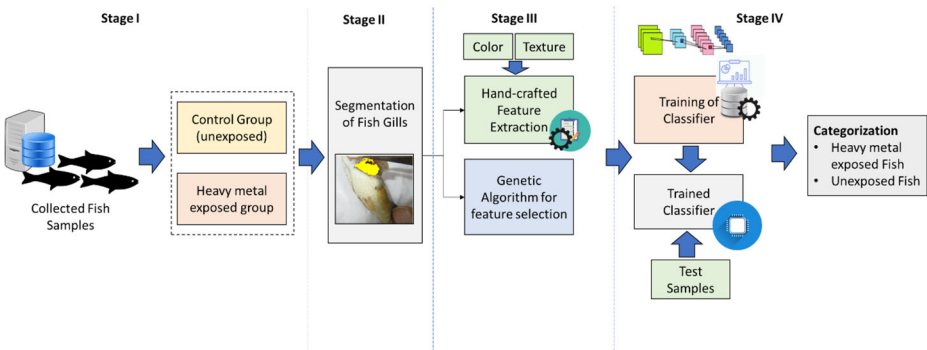


Fig. 2 Block diagram of the proposed methodology

When an image in the RGB color model is transformed into the YCbCr color model, the resultant image consists of an intensity component (Y) and chrominance components (Cb and Cr). Figure 3 visualises the R, G and B component images for the RGB color model and the Y, Cb and Cr component images for the YCbCr color model for a randomly chosen fish sample image. It can be visualised from Fig. 3 that for the given sample image the gill region is most highlighted in the Cr component image; therefore, it is the best-suited component for the segmentation of the gill area using the proposed segmentation algorithm.

**The proposed segmentation algorithm** The YCbCr color model also provides better color clustering performance. Therefore, after selecting the Cr plane image center initialised K-means clustering algorithm is used to segment the pre-processed chrominance channel gill image. The proposed algorithm converges faster in comparison to the random initialisation of the center-based approach.

**Input:** A Chrominance (Cr) component image of YCbCr model.

**Procedure:**

Pre-set the total number of clusters ( $k = 4$ ) and choose their values in such a manner, that the entire range of grey scale is divided into five equal parts so that it is equally spaced over the entire range of grey levels in an image. Now measure the euclidean distance between the cluster centres and the rest of the pixel values present in an image using Eq. (2).

$$d_{x,y} = f(x,y) - c_k \tag{2}$$

where,  $d_{x,y}$  is the distance of the pixel at coordinates x and y from the  $k^{th}$  cluster centre  $c_k$ .

Assign pixel to cluster which is nearest to that pixel based on Euclidean distance d from the cluster centre  $c_k$ . After assigning all the pixels to their nearest cluster, cluster centres are recalculated using the relation using Eq. (3):

$$c_k = \frac{\sum_{i=1}^n f_i(x,y)}{n} \tag{3}$$

where, n denotes total number of pixels in a cluster centred around  $c_k$ . Repeat the last three steps till the cluster centres stop changing their positions.

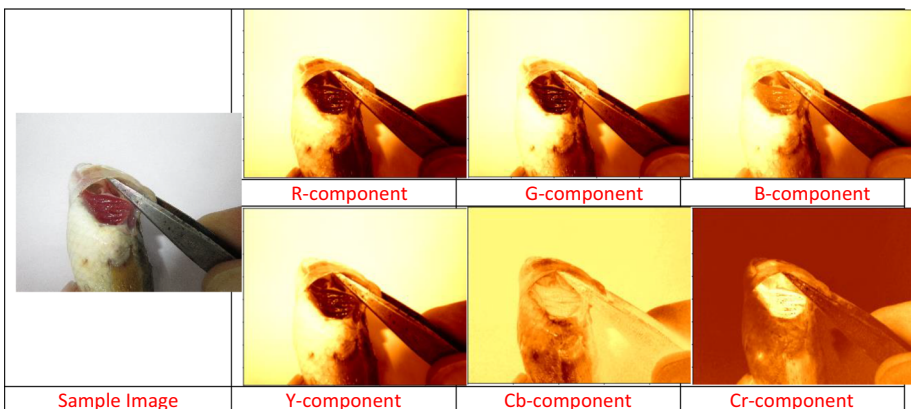


**Fig. 3** Visualisation of an image of individual components of the RGB color model (first row) and YCbCr color model (second row)

**Output:** Segmented image.

The image formed by the fourth cluster is chosen for morphological post-processing, where hole-filling and area-based object selection procedure is used to remove the noise. The segmented gill images obtained after applying the proposed segmentation algorithm is shown in Fig. 4 which shows the good extraction of ROI for a given input image.

Post segmentation the features are extracted from the gill region using color and texture features.

### 3.2.2 Suitable feature representation for segmented gill image

The discriminative features are drawn out from the segmented gill region of the fish sample by giving the segmented gill image as input to the proposed feature extraction procedure. Suitable color and texture features were extracted and further optimised for better performance using a genetic algorithm.

**The proposed feature extraction process** Many studies have validated the change in colour and physical parameters of fish and their organs due to exposure to heavy metals [21, 36, 40, 45, 57, 58]. Since the accumulation of heavy metal residues occurs in fish gills, therefore, it may bring changes to the color and texture features of the heavy-metal exposed fish gills. It was observed during experiments that neither color nor texture features can individually classify the fish samples in the control and experimental group with high accuracy, therefore the combination of color and texture features has been used to classify the fish samples in the control and metal-exposed class.

In the present work, color features have been extracted using the first two-colour moments, i.e., the mean and standard deviation. The color-moments represent the distribution of color in an image. The color moments have been extracted from the red channel of the RGB (Red-Green-Blue) color model, the hue channel of the HSI (Hue-Saturation-Intensity) color model and the chrominance (Cr) channel of the YCbCr color model. The reason for choosing these channels is the dominance of red color in the image of the segmented fish-gill region. The mean and standard deviation can be calculated from each of the channels using Eq. (4) and (5) respectively.

$$mean = \frac{1}{mn} \sum_{i=1}^{i=m} \sum_{j=1}^{j=n} f_{ij} \quad (4)$$

$$Std.dev = \sqrt{\frac{\sum_{i=1}^{i=m} \sum_{j=1}^{j=n} (f_{ij} - mean)^2}{(m-1)(n-1)}} \quad (5)$$

where,  $f_{ij}$  is the pixel intensity at  $i^{th}$  row and  $j^{th}$  column and mean is the average intensity value of a 2D image having m rows and n columns. The texture features from the segmented region are extracted using the Local Binary Pattern (LBP). The calculation of LBP code for a specific pixel is performed using Eq. (6):

$$LBP_{N,R}(f_c) = \sum_{N=0}^{N-1} g(f_N - f_c) \cdot 2^N \quad (6)$$



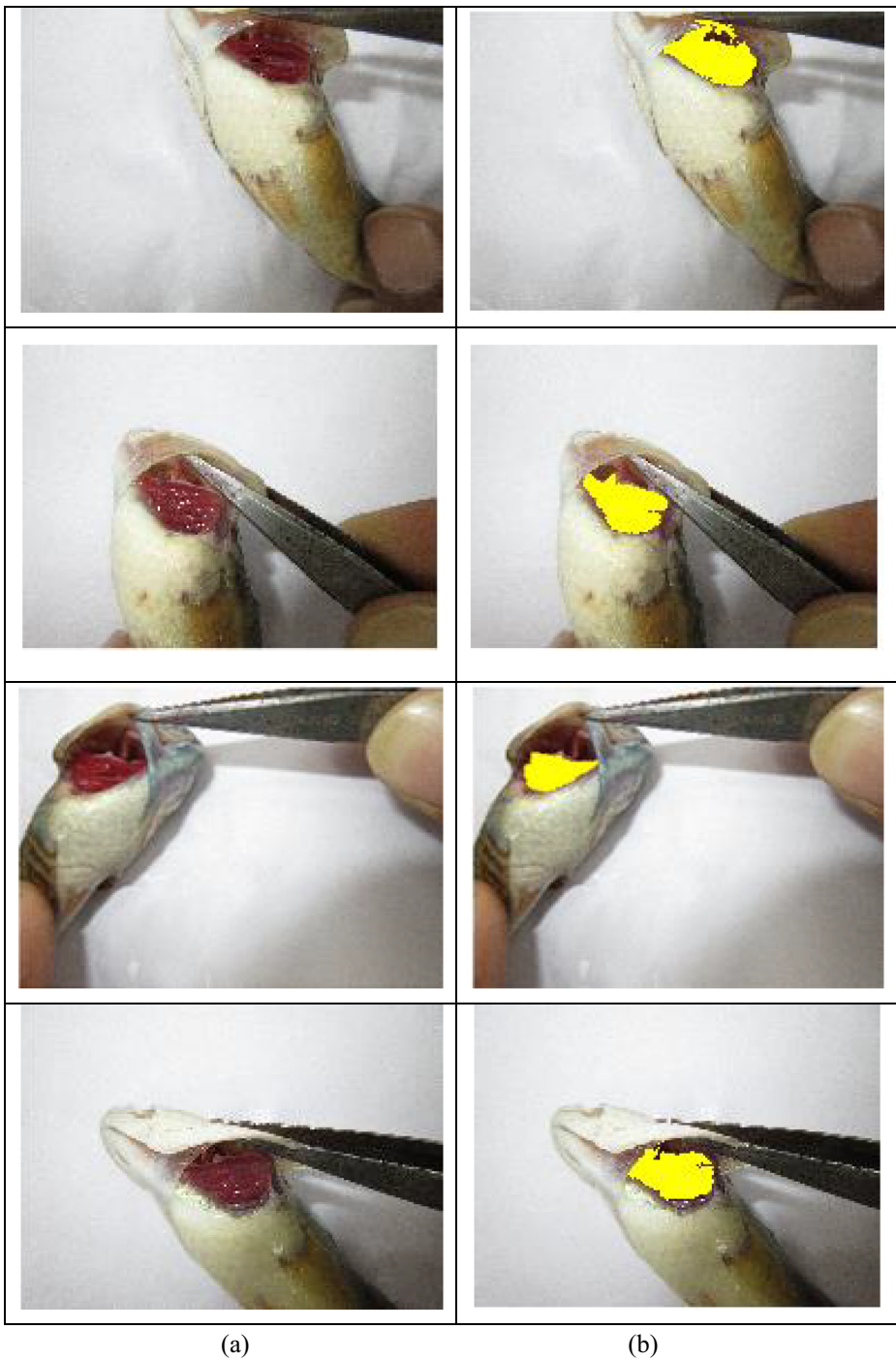


**Fig. 4** The output of the fish gill segmentation (a) Displays the original colour images and (b) Highlights the segmented region of the fish gill (in yellow)

where,  $f_c$  is the value of the central pixel and  $f_N$  ( $N = 0, 1, 2, \dots, N - 1$ ) is the value of pixels located at the neighbourhood of radius  $R$  and  $N$  is the number of sampled neighbours. And  $g(x) = 1$  for  $x > 0$ , otherwise,  $g(x) = 0$ . In this work, uniform LBP pattern [60] has been utilised since it reduces the size of the feature vector by only selecting those patterns which have a limited number ( $\leq 2$ ) of bit transitions from 0 to 1 or 1 to 0 and grouping all non-uniform patterns (no. of transitions  $> 2$ ) into a single category. The uniform patterns are approximately accounted for 80% of the patterns present in any texture image [60]. With  $N$  ( $=8$ ) neighbourhood pixels total  $N*(N-1) + 2$  ( $=58$ ) different uniform bit patterns are possible. The transformation from simple LBP to uniform LBP is implemented using a lookup table having  $2^N$  entries mapping 58 different bit patterns. All uniform patterns have been shown in Fig. 5. All patterns in one row, as shown in Fig. 5, can be normalised to single pattern, therefore, total 9 patterns are possible after converting uniform patterns into rotation invariant LBP operator, denoted by  $LBP^{riu}$ .

Thus, the total number of features in case of uniform LBP and rotation invariant LBP patterns when combined with the proposed color descriptors were 64 and 15 respectively. Since a large number of features affects the performance of a classifier due to the curse of dimensionality and may also result in overfitting. Therefore, the selection of highly discriminatory features is of utmost importance as it will not only reduce the complexity of a classifier but it will also improve its accuracy.

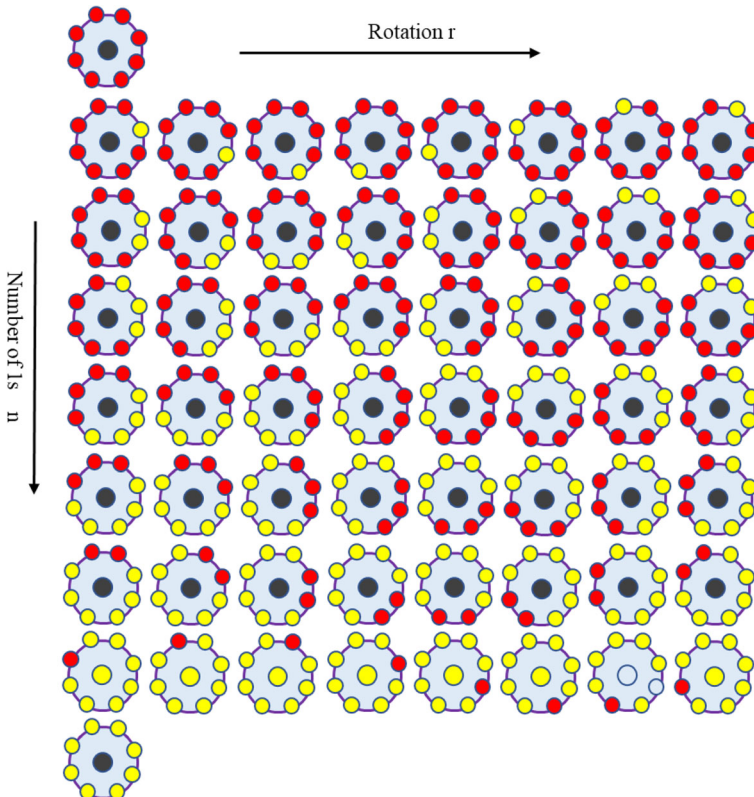


Fig. 5 Different uniform local binary patterns formed for #Neighbor = 8, radius = 1

### 3.2.3 Feature selection using genetic algorithm

The most discriminatory features were selected using the genetic algorithm. Binary encoding has been used to encode the features. The features are selected based on the fitness measure defined for the genetic algorithm. The fitness measure used for the genetic algorithm is defined using Eq. (7):

$$cost_i = w_1 * error(z_i) + w_2 * r_f \quad (7)$$

where,  $w_1$  and  $w_2$  are the weightage assign to the component of Eq. (7). These value for these weightages ranging from 0 to 1; whereas,  $w_2 = w_1 - 1$ ;  $r_f$  is the ratio of the length of the selected feature to the total number of features;  $cost_i$  is a cost function of  $i^{th}$  selected feature for a given classifier; Cost function has two sub-component: first part of the cost function represents the weighted classification accuracy of a classifier on  $i^{th}$  selected feature subset (chromosome) represented by  $z_i$  and the second part of the Eq. (7) represents the weighted ratio of the length of selected feature. Generally,  $w_1$  can vary from 0.75 to 1 based on user requirements. If accuracy is more important than feature reduction then  $w_1$  is given more weightage than  $w_2$ . The value of  $w_1 = 0.80$  and  $w_2 = 0.20$  is used for experiments in the proposed work.

### 3.2.4 Framework for classification

The extracted-reduced features from the earlier two approaches were used to train different machine learning classifiers; the training parameters for these classifiers are shown in Table 2.

## 4 Experimental results

In this work, NVIDIA Tesla K40 GPU (12 GB RAM) has been used for execution purpose with implementation of all the methods on Python 3.5. Different performance metrics are used to assess the performance of the proposed method such as precision, recall, F1-score and AUC (Area under the curve). The experimental results for the proposed method have been presented in section 4.1 and the experimental results obtained with the transfer learning-based method have been presented in section 4.2.

### 4.1 Classification performance of the proposed genetically optimised color texture features-based approach

This section describes the experimental results obtained from the training of a classifier with hand-crafted color and texture features and the improvement in classifier performance before and after the selection of features using a genetic algorithm.

**Table 2** Training parameters of different classifiers

Machine Learning Model	Parameters settings for classification
Support Vector Machine	Gaussian Radial Basis Function Kernel, Scaling Factor Sigma=1.8
Artificial Neural Network	No. of Hidden Layers=5, Training Function=Levenberg-Marquardt, Epochs=30
Random Forest	Number of trees=40

**Table 3** Feature selected by genetic algorithm for different classifiers and the accuracy of a classifier with selected features

Classifier	#color and texture features	Accuracy	#features by the genetic algorithm	Accuracy (%)
SVM	64	92.14	9	96.4
Neural Network	64	96.15	11	95.7
Random Forest	64	97.04	32	97.1

Table 3 represents the total number of features before and after feature selection using a genetic algorithm and the corresponding accuracy of the prediction of the classifier. It can be analysed from Table 3 that the accuracy of SVM and Random Forest classifiers improves with a significant reduction in several features. Among all the classifiers Random Forest performs well in terms of accuracy.

After applying the genetic algorithm and selection of discriminatory features, the average performance metrics of the trained SVM classifier such as recall, precision, F-score and accuracy are evaluated using a five-fold cross-validation technique for the proposed method have been shown in Table 4. The Random Forest classifier performs the best among other mentioned classifiers with an AUC score of 0.98 while the Neural Network classifier performance is the worst and achieved an AUC score of 0.94.

The average computation time is 1.34 seconds for processing each image using the proposed methodology. Figure 6 shows the mean ROC curve for the 5-folds for different classifiers before and after the selection of features. It can be analysed from the ROC curves of the classifier that the performance of the classifier gets improved for all the classifiers except Neural Network.

A comparison between the classification performance of the SVM classifier obtained with different LBP descriptors when these features were combined with the proposed color descriptors has also been made and presented in Table 5. The number of features pre and post-selection and the corresponding classification accuracy obtained with each LBP-based descriptor has also been presented in Table 5.

It can be analysed from the Table 5 that rotation invariant LBP has given better performance in comparison to other LBP descriptors.

## 4.2 Comparison of the proposed method with the transfer learning-based approach

Pre-trained deep CNN models such as VGG16 [52], Resnet50 [23], Inception v3 [55], Mobilenet [18] are used for feature extraction. The last convolution layer of different pre-trained deep CNN models is used to draw out feature maps from an input image (RGB format) of size  $224 \times 224 \times 3$ . Before drawing out the features from the gill, it is segmented out. These feature maps were further given as an input to the global average pooling (GAP) layer to

**Table 4** Performance measurement of classifiers with feature selection

Model	Recall	Precision	F- score	Accuracy	AUC
Support Vector Machine	1	0.928	0.965	0.964	0.95
Neural Network	0.932	0.985	0.957	0.957	0.94
Random Forest	0.971	0.971	0.971	0.971	0.98

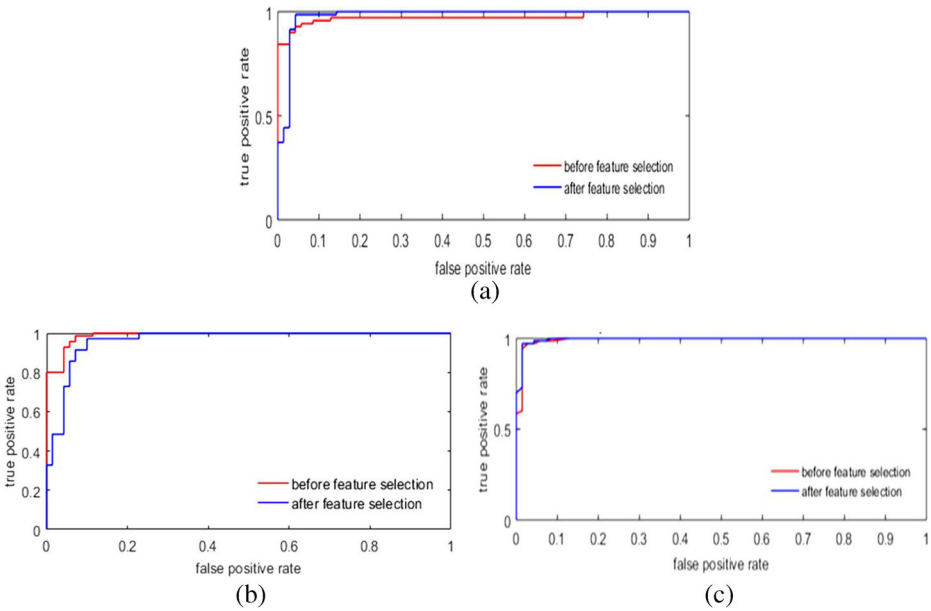


**Fig. 6** Mean ROC curve for 5-folds of the classifiers before and after features selection for different classifiers (a) SVM (b) Neural Network (c) Random Forest

obtain concise global representation of the features present in an input image. The output of the GAP layer is used to train SVM classifier for discriminating heavy-metal exposed and non-exposed fish.

**4.2.1 Classification performance of the transfer learnt SVM classifier**

The average performance metrics of the SVM classifier trained with the features drawn out from the pre-trained CNNs for five-fold cross-validation have been shown in Table 6. As shown in Table 6, VGG16-based features outperforms with an average classification accuracy of 93.5% for SVM. The highest value of precision and recall was obtained with the features of the VGG16 model. The discriminability of features drawn out from different pre-trained models can be ranked based on the performance of SVM classifier as shown in Table 6.

ROC curves for each of the 5 folds for trained SVM on features drawn out from the pre-trained model are shown in Fig. 7, where the mean area under the curve (AUC) was maximum for the VGG16 model whereas it was minimum for the Inception v3 model.

**Table 5** Classification performance obtained with different LBP descriptors and the number of selected features

Descriptor	#features before selection	#features selected	SVM classifier %accuracy with selected features
LBP	262	18	89.1
Uniform LBP	64	9	96.4
Rotation-invariant LBP	15	8	96.4

**Table 6** Performance metrics for SVM on features extracted from pre-trained deep CNN models

Model	Recall	Precision	F- score	Accuracy	AUC
VGG16	0.937	0.937	0.937	0.935	0.99
Resnet50	0.823	0.875	0.848	0.843	0.94
Inceptionv3	0.769	0.714	0.741	0.750	0.84
Mobilenet	0.75	0.643	0.692	0.714	0.89

The performance of SVM with the features drawn out from different pre-trained CNNs, is almost uninterpretable. Since these deep models were trained on the ImageNet dataset which consists of millions of images of almost 1000 categories it has nothing to do with the presence of heavy metal traces in the fish gills. Therefore, certain hand-crafted features were explored to establish a discrimination between the fish samples of exposed and non-exposed groups. The performance of machine learning models on these hand-crafted features is explained in the next subsection.

#### 4.2.2 Visualisation of the learned features using saliency-based techniques

It has been investigated and attempted to visualise the learned features using a saliency-based method [46] as shown in Fig. 8. However, due to the drawback of saliency-based methods as highlighted in [1] that sometimes these methods work independently of features learnt by the

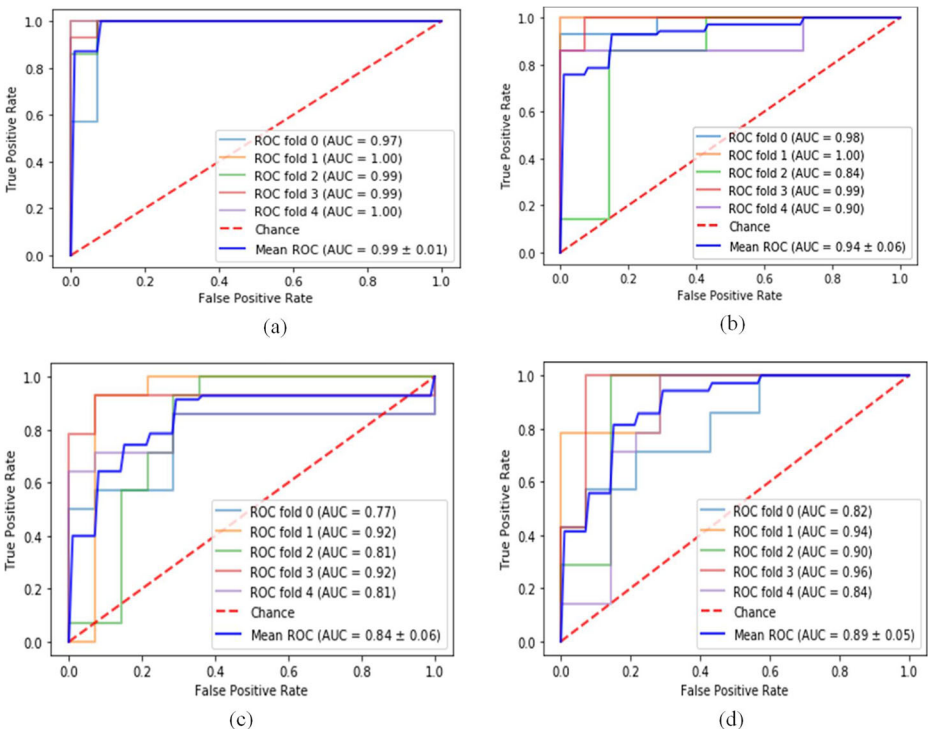


**Fig. 7** ROC curves for 5 folds on features extracted from (a) VGG16 (b) Resnet50 (c) Inception v3 (d) Mobilenet

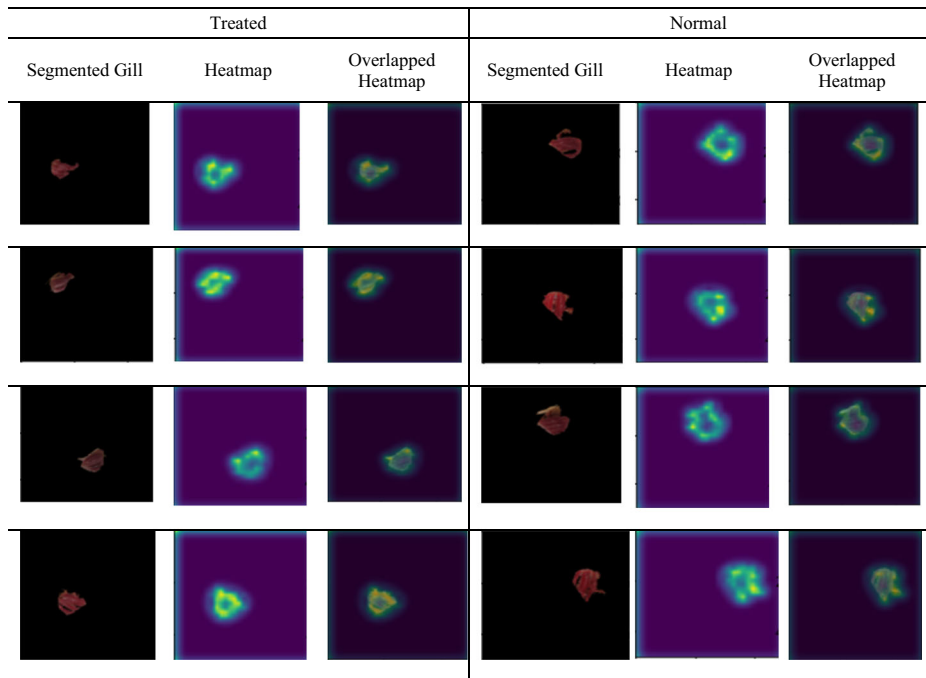


**Fig. 8** Visualisation of gradients of the last convolution layer for class score (GradCAM saliency method)

model and simply work as an edge detector. The same observation has been made in our case as saliency-based techniques cannot highlight the salient regions in an input image and work only as an edge detector. The reason for this drawback is that the gradients are calculated only for the weights learnt by the model from the last convolution layer, not for the weights learnt by the model in all other convolution layers present in the CNN. As shown in Fig. 8 that the saliency-based method only highlights the edges of a gill region present in an image which may not be the case as the exposure of heavy metals to fish bring changes in the textural and color properties of its gill region which has also been established with the experimental results presented in section 5.2.

## 5 Comparison with the other similar approaches

The methods earlier developed for the fish quality assessment have been described in brief with the conclusion in Table 7 and also compared with the present proposed method.

**Table 7** Comparison of state-of-the-art works and proposed work

S. No.	Work No.	Year	Short description	Methodology used	Dataset description	Experimental results
1	[47]	2017	To identify pesticide exposure in fish	Wavelet domain features were extracted from the fish gill for the classification of cypermethrin-exposed fish.	Out of 144 images of the pesticide-exposed and non-exposed group fish, 80 images were utilised for training purpose and 64 images were used for testing purpose.	Classification accuracy of 95% was achieved with the SVM.
2	[53]	2017	To identify the drug-induced deformation in Zebrafish	The deep learning technique has been used for the classification of deformed and normal Zebrafish.	5fold cross-validation has been applied for the classification of deformed and normal Zebrafish, using 3folds (84 images) for training, 1fold (28 images) for validation and 1fold (28 images) for testing, in each 5-fold split	92.8% accuracy on unseen test-data
3	[27]	2019	To identify heavy metal exposure in fish	A mathematical parameter was derived from the biomarker present in the heavy-metal exposed fish eye	A total of 116 fish samples were used to capture the left and right eye images for each fish for formulating the proposed mathematical parameter	The biomarker present in the fish eye was validated with the ground truth.
4	[53]	2021	To identify heavy metal exposure in fish	Image processing and machine learning techniques	Out of 110 fish sample images 80% were used for training and 20% were used for testing	The best classification accuracy was achieved at 87.02%.
5	Proposed work	2021	To classify the heavy metal exposed and non-exposed food fish machine/deep learning	The discriminatory features were extracted and classified using the deep learning/ machine learning technique.	5-fold cross validation procedure has been used in which 4 folds (88 sample images) were used for training purpose and the remaining fold (22 sample images) were used for the testing purpose, in each split	The best classification accuracy of 97.1% was obtained on unseen-test data



## 6 Conclusions and future work

The present work successfully developed a machine-learning-based method for the categorisation of heavy metal exposed and non-exposed fish using the gill tissue of the fish as a region of interest. The proposed methodology has been analysed in multiple sets of configurations and techniques. The color and texture features extracted from the segmented gill region gives better discrimination ability in comparison to the features extracted from the transfer learnt deep features extracted from pre-trained deep convolution neural networks. The color texture features after optimising using genetic algorithm give better classification performance. The methodology proposed in the present work is easy to implement in that it can be used for the classification of heavy-metal exposed fish at a commercial scale with almost no incurred cost. Large image datasets related to the fish and the effect of other heavy metals will be analysed in future work to assess the impact of heavy metals in a more efficient manner.

**Data availability** The datasets generated during and/or analysed during the current study are available from the corresponding author on reasonable request.

### Declaration

**Conflicting interests** The authors declared no potential conflicts of interest with respect to the research, authorship, and/or publication of this article

**Ethical clearance** In our knowledge, as per the Indian laws, working with food fish, does not require ethical clearance.

## References

1. Adebayo J, Gilmer J, Muelly M et al (2018) Sanity checks for saliency maps. *Advances in Neural Information Processing Systems*, In
2. Amakdouf H, Zouhri A, El Mallahi M et al (2021) Artificial intelligent classification of biomedical color image using quaternion discrete radial Tchebichef moments. *Multimed Tools Appl* 80:3173–3192. <https://doi.org/10.1007/s11042-020-09781-x>
3. Authman MMN, Abbas HH, Abbas WT (2013) Assessment of metal status in drainage canal water and their bioaccumulation in *Oreochromis niloticus* fish in relation to human health. *Environ Monit Assess* 185:891–907. <https://doi.org/10.1007/s10661-012-2599-8>
4. Banwari A, Joshi RC, Sengar N, Dutta MK (2022) Computer vision technique for freshness estimation from segmented eye of fish image. *Ecol Inform* 69:101602
5. Bose MTJ, Ilavazhahan M, Tamilselvi R, Viswanathan M (2013) Effect of heavy metals on the histopathology of gills and brain of fresh water fish *Catla catla*. *Biomed Pharmacol J* 6:99–105. <https://doi.org/10.13005/bpj/390>
6. Boyd CE (2005) LC 50 calculations help predict toxicity. *Glob Aquac Advocate*, p 84,87
7. Chandra Joshi R, Mishra R, Gandhi P, ... Dutta MK (2021) Ensemble based machine learning approach for prediction of glioma and multi-grade classification. *Comput Biol Med* 137:104829. <https://doi.org/10.1016/j.combiomed.2021.104829>
8. Cheng JH, Dai Q, Sun DW, ... Pu HB (2013) Applications of non-destructive spectroscopic techniques for fish quality and safety evaluation and inspection. *Trends Food Sci Technol* 34:18–31
9. Ching T, Himmelstein DS, Beaulieu-Jones BK, ... Greene CS (2018) Opportunities and obstacles for deep learning in biology and medicine. *J R Soc Interface* 15:20170387. <https://doi.org/10.1098/rsif.2017.0387>
10. de Souza Hacon S, Oliveira-da-Costa M, de Souza Gama C et al (2020) Mercury exposure through fish consumption in traditional communities in the Brazilian northern Amazon. *Int J Environ Res Public Health* 17:5269. <https://doi.org/10.3390/ijerph17155269>

11. de Souza Hacon S, Oliveira-da-Costa M, de Souza Gama C et al (2020) Mercury exposure through fish consumption in traditional communities in the Brazilian northern Amazon. *Int J Environ Res Public Health* 17:5269. <https://doi.org/10.3390/ijerph17155269>
12. de Vasconcellos ACS, Hallwass G, Bezerra JG et al (2021) Health risk assessment of mercury exposure from fish consumption in Mundurucu indigenous communities in the Brazilian Amazon. *Int J Environ Res Public Health* 18:7940. <https://doi.org/10.3390/ijerph18157940>
13. Dhanakumar S, Salaraj G, Mohanraj R (2015) Heavy metal partitioning in sediments and bioaccumulation in commercial fish species of three major reservoirs of river Cauvery delta region, India. *Ecotoxicol Environ Saf* 113:145–151. <https://doi.org/10.1016/j.ecoenv.2014.11.032>
14. Djedjibegovic J, Marjanovic A, Tahirovic D, ... Caklovica F (2020) Heavy metals in commercial fish and seafood products and risk assessment in adult population in Bosnia and Herzegovina. *Sci Rep* 10:13238. <https://doi.org/10.1038/s41598-020-70205-9>
15. Dowlati M, de la Guardia M, Dowlati M, Mohtasebi SS (2012) Application of machine-vision techniques to fish-quality assessment. *TrAC - Trends Anal, Chem*
16. Dowlati M, Mohtasebi SS, Omid M, ... de la Guardia M (2013) Freshness assessment of gilthead sea bream (*Sparus aurata*) by machine vision based on gill and eye color changes. *J Food Eng* 119:277–287. <https://doi.org/10.1016/j.jfoodeng.2013.05.023>
17. Dutta MK, Issac A, Minhas N, Sarkar B (2016) Image processing based method to assess fish quality and freshness. *J Food Eng* 177:50–58. <https://doi.org/10.1016/j.jfoodeng.2015.12.018>
18. Ekoputris RO (2018) MobileNet: Deteksi Objek pada Platform Mobile. 9 May 2018
19. Fazio F, Piccione G, Tribulato K, ... Faggio C (2014) Bioaccumulation of heavy metals in blood and tissue of striped mullet in two Italian Lakes. *J Aquat Anim Health* 26:278–284. <https://doi.org/10.1080/08997659.2014.938872>
20. Fu Z, Xi S (2020) The effects of heavy metals on human metabolism. *Toxicol Mech Methods* 30(3):167–176. <https://doi.org/10.1080/15376516.2019.1701594>
21. Georgieva E, Velcheva I, Yancheva V, Stoyanova S (2014) Trace metal effects on gill epithelium of common carp *Cyprinus carpio* L. (cyprinidae) *Acta Zool. Bulgarica*. 66:277–282
22. Hashim R, Song TH, Muslim NZM, Yen TP (2014) Determination of heavy metal levels in fishes from the lower reach of the Kelantan River, Kelantan, Malaysia. *Trop life Sci Res* 25:21–39
23. He K, Zhang X, Ren S, Sun J (2016) Identity mappings in deep residual networks. In: lecture notes in computer science (including subseries lecture notes in artificial intelligence and lecture notes in bioinformatics).
24. Huseen HM, Mohammed AJ (2019) Heavy metals causing toxicity in fishes. *J Phys Conf Ser* 1294:62028. <https://doi.org/10.1088/1742-6596/1294/6/062028>
25. Isangedighi IA, David GS (2019) Heavy metals contamination in fish: effects on human health. *J Aquatic Sci Marine Biol* 2:7–12
26. Ishaq O et al (2017) Deep fish. *SLAS Discovery: Advancing Life Sciences R & D* 22(1):102–107. <https://doi.org/10.1177/1087057116667894>
27. Issac A, Srivastava A, Srivastava A, Dutta MK (2019) An automated computer vision based preliminary study for the identification of a heavy metal (hg) exposed fish-*channa punctatus*. *Comput Biol Med* 111: 103326. <https://doi.org/10.1016/j.combiomed.2019.103326>
28. Järup L (2003) Hazards of heavy metal contamination. *Br Med Bull* 68:167–182. <https://doi.org/10.1093/bmb/ldg032>
29. Javed M, Usmani N (2019) An overview of the adverse effects of heavy metal contamination on fish health. *Proc Natl Acad Sci India Sect B Biol Sci* 89:389–403. <https://doi.org/10.1007/s40011-017-0875-7>
30. Joshi RC, Joshi M, Singh AG, Mathur S (2018) Object detection, classification and tracking methods for video surveillance: a review. In: 2018 4th international conference on computing communication and automation, ICCCA 2018.
31. Kawser Ahmed M, Baki MA, Kundu GK, ... Muzammel Hossain M (2016) Human health risks from heavy metals in fish of Buriganga river, Bangladesh. *Springerplus* 5:1697. <https://doi.org/10.1186/s40064-016-3357-0>
32. Lim JW, Kim TY, Woo MA (2021) Trends in sensor development toward next-generation point-of-care testing for mercury. *Biosens Bioelectron* 183:113228
33. Ling H, Wu J, Huang J, ... Li P (2020) Attention-based convolutional neural network for deep face recognition. *Multimed Tools Appl* 79:5595–5616. <https://doi.org/10.1007/s11042-019-08422-2>
34. Litjens G, Kooi T, Bejnordi BE, ... Sánchez CI (2017) A survey on deep learning in medical image analysis. *Med Image Anal* 42:60–88
35. Maier D, Blaha L, Giesy JP, ... Triebeskorn R (2015) Biological plausibility as a tool to associate analytical data for micropollutants and effect potentials in wastewater, surface water, and sediments with effects in fishes. *Water Res* 72:127–144. <https://doi.org/10.1016/j.watres.2014.08.050>


36. Mathivanan R (2004) Effects of sublethal concentration of quinophos on selected respiratory and biochemical parameters in the fresh water fish *Oreochromis mossambicus*. *J Ecotoxicol Environ Monit* 14(1):57–64
37. Maurya PK, Malik DS, Yadav KK, ... Kamyab H (2019) Bioaccumulation and potential sources of heavy metal contamination in fish species in river ganga basin: possible human health risks evaluation. *Toxicol Reports* 6:472–481. <https://doi.org/10.1016/j.toxrep.2019.05.012>
38. Mehmood MA, Qadri H, Bhat RA, ... Shafiq-ur-Rehman (2019) Heavy metal contamination in two commercial fish species of a trans-Himalayan freshwater ecosystem. *Environ Monit Assess* 191:104. <https://doi.org/10.1007/s10661-019-7245-2>
39. Min S, Lee B, Yoon S (2017) Deep learning in bioinformatics. *Brief Bioinform*
40. Oliveira Ribeiro CA, Vollaire Y, Sanchez-Chardi A, Roche H (2005) Bioaccumulation and the effects of organochlorine pesticides, PAH and heavy metals in the eel (*Anguilla anguilla*) at the Camargue nature reserve. *France Aquat Toxicol* 74:53–69. <https://doi.org/10.1016/j.aquatox.2005.04.008>
41. Poleksic V, Lenhardt M, Jaric I, ... Raskovic B (2010) Liver, gills, and skin histopathology and heavy metal content of the Danube sterlet (*Acipenser ruthenus* Linnaeus, 1758). *Environ Toxicol Chem* 29:515–521. <https://doi.org/10.1002/etc.82>
42. Rehman K, Fatima F, Waheed I, Akash MSH (2018) Prevalence of exposure of heavy metals and their impact on health consequences. *J Cell Biochem* 119(1):157–184. <https://doi.org/10.1002/jcb.26234>
43. Roméo M, Siau Y, Sidoumou Z, Gnassia-Barelli M (1999) Heavy metal distribution in different fish species from the Mauritania coast. *Sci Total Environ* 232:169–175. [https://doi.org/10.1016/S0048-9697\(99\)00099-6](https://doi.org/10.1016/S0048-9697(99)00099-6)
44. Romero-Romero S, García-Ordiales E, Roqueñí N, Acuña JL (2022) Increase in mercury and methylmercury levels with depth in a fish assemblage. *Chemosphere* 292:133445. <https://doi.org/10.1016/j.chemosphere.2021.133445>
45. Santhakumar M, Balaji M (2000) Acute toxicity of an organophosphorus insecticide monocrotophos and its effects on behaviour of an air-breathing fish, *Anabas testudineus* (Bloch). *J Environ Biol* 21(2):121–123
46. Selvaraju RR, Cogswell M, Das A et al (2020) Grad-CAM: visual explanations from deep networks via gradient-based localization. *Int J Comput Vis* 128:336–359. <https://doi.org/10.1007/s11263-019-01228-7>
47. Sengar N, Dutta MK, Sarkar B (2017) Computer vision based technique for identification of fish quality after pesticide exposure. *Int J Food Prop*:1–15. <https://doi.org/10.1080/10942912.2017.1368553>
48. Sengar N, Gupta V, Dutta MK, Travieso CM (2018) Image processing based method for identification of fish freshness using skin tissue. In: 2018 4th international conference on Computational Intelligence & Communication Technology (CICT), pp 1–4
49. Sfakianakis DG, Renieri E, Kentouri M, Tsatsakis AM (2015) Effect of heavy metals on fish larvae deformities: a review. *Environ Res* 137:246–255. <https://doi.org/10.1016/j.envres.2014.12.014>
50. Sharma K, Sharma P, Dhiman SK, ... Saini HS (2022) Biochemical, genotoxic, histological and ultrastructural effects on liver and gills of fresh water fish *Channa punctatus* exposed to textile industry intermediate 2 ABS. *Chemosphere* 287:132103. <https://doi.org/10.1016/j.chemosphere.2021.132103>
51. Shen J, Robertson N (2021) BBAS: towards large scale effective ensemble adversarial attacks against deep neural network learning. *Inf Sci (Ny)* 569:469–478. <https://doi.org/10.1016/j.ins.2020.11.026>
52. Simonyan K, Zisserman A (2015) Very deep convolutional networks for large-scale image recognition. In: 3rd international conference on learning representations, ICLR 2015 - conference track proceedings.
53. Singh A, Gupta H, Srivastava A, ... Dutta MK (2021) A novel pilot study on imaging-based identification of fish exposed to heavy metal (hg) contamination. *J Food Process Preserv* 45. <https://doi.org/10.1111/jfpp.15571>
54. Swain KK, Balasubramaniam R, Bhand S (2020) A portable microfluidic device-based Fe3O4-urease nanoprobe-enhanced colorimetric sensor for the detection of heavy metals in fish tissue. *Prep Biochem Biotechnol* 50:1000–1013. <https://doi.org/10.1080/10826068.2020.1780611>
55. Szegedy C, Liu W, Jia Y, et al (2015) Going deeper with convolutions. In: Proceedings of the IEEE Computer Society Conference on Computer Vision and Pattern Recognition
56. Taweel AKA, Shuhaimi-Othman M, Ahmad AK (2012) Analysis of heavy metal concentrations in tilapia fish (*Oreochromis niloticus*) from four selected markets in Selangor. *Peninsular Malaysia J Biol Sci*. <https://doi.org/10.3923/jbs.2012.138.145>
57. Vasanthi N, Muthukumaravel K, Sathick O, Sugumaran J (2019) Toxic effect of mercury on the freshwater fish *Oreochromis mossambicus*. *Res J life Sci Bioinform Pharm Chem Sci* 5(3):365–376Page 23/31. <https://doi.org/10.26479/2019.0503.30>
58. Vinodhini R, Narayanan M (2009) Heavy metal induced histopathological alterations in selected organs of the *Cyprinus carpio* L. (common carp). *Int J Environ Res*. <https://doi.org/10.22059/ijer.2009.35>
59. Wang L, Qian X, Zhang Y, ... Cao X (2020) Enhancing sketch-based image retrieval by CNN semantic re-ranking. *IEEE Trans Cybern* 50:3330–3342. <https://doi.org/10.1109/TCYB.2019.2894498>

60. Xia S, Chen P, Zhang J, Li X, Wang B (2017) Utilization of rotation-invariant uniform LBP histogram distribution and statistics of connected regions in automatic image annotation based on multi-label learning. *Neurocomputing* 228:11–18. <https://doi.org/10.1016/j.neucom.2016.09.087>

**Publisher's note** Springer Nature remains neutral with regard to jurisdictional claims in published maps and institutional affiliations.

Springer Nature or its licensor (e.g. a society or other partner) holds exclusive rights to this article under a publishing agreement with the author(s) or other rightsholder(s); author self-archiving of the accepted manuscript version of this article is solely governed by the terms of such publishing agreement and applicable law.

## Affiliations

Ritesh Maurya<sup>1</sup> · Arti Srivastava<sup>2</sup> · Ashutosh Srivastava<sup>2,3</sup> · Vinay Kumar Pathak<sup>4</sup> · Malay Kishore Dutta<sup>5</sup> 

Ritesh Maurya  
maurya123rites47@gmail.com

Arti Srivastava  
asrivastava@amity.edu

Ashutosh Srivastava  
asrivastava4@amity.edu

Vinay Kumar Pathak  
vinay@vpathak.in

<sup>1</sup> Department of Information Technology, Manipal Institute of Technology Bengaluru, Manipal Academy of Higher Education, Manipal, India

<sup>2</sup> Amity Institute of Biotechnology, Amity University, Noida, U.P., India

<sup>3</sup> Amity Institute of Marine Science and Technology, Amity University, Noida, U.P., India

<sup>4</sup> Chhatrapati Shahu Ji Maharaj University, Kanpur, U.P., India

<sup>5</sup> Centre of Advanced Studies, Dr. A. P. J. Abdul Kalam Technical University, Lucknow, U.P., India